Preparation and Characterization of Cellulose-based Composite Films Using Pyridinium-based Ionic Liquids

Temmy Pegarro Vales
Department of Chemistry, Caraga State University

Evelyn C. Creencia
Department of Chemistry, Mindanao State University - Iligan Institute of Technology

https://doi.org/10.5109/7395638

出版情報：Proceedings of International Exchange and Innovation Conference on Engineering & Sciences (IEICES). 11, pp.1021-1028, 2025-10-30. International Exchange and Innovation Conference on Engineering & Sciences
バージョン：

Preparation and Characterization of Cellulose-based Composite Films Using Pyridinium-based Ionic Liquids

Temmy Pegarro Vales[1,2] and Evelyn C. Creencia[3]
[1] Department of Chemistry, Caraga State University, Butuan, Agusan del Norte 8600 Philippines
[2] Mineral Resources Management Research and Training Center, Caraga State University, Butuan, Agusan del Norte 8600 Philippines
[3] Department of Chemistry, Mindanao State University – Iligan Institute of Technology, Iligan City 9200 Philippines
tpvales@carsu.edu.ph

Abstract: *A series of Br-based ionic liquids (ILs) were synthesized from pyridine and alkyl bromides, yielding 9.56% to 97.49%, with product efficiency influenced by alkyl chain length and branching. Subsequent anion exchange of 1-butylpyridinium bromide with sodium acetate at 130 °C enhanced conversion, reaching 94.49%. Using [n-C4py]Br, cellulose-based composite films were prepared sustainably. Structural characterization such as Fourier Transform Infrared spectroscopy (FT-IR) and Scanning Electron Microscopy with Energy-Dispersive X-ray Spectroscopy (SEM-EDS) confirmed effective starch and activated carbon incorporation. Starch-enhanced films (up to 30 wt%) showed improved mechanical properties and more ordered morphology, whereas activated carbon caused poor adhesion and flake-like structures. Antimicrobial activity testing via Paper Disc Diffusion showed no significant inhibition against various bacterial and fungal strains, including Candida albicans, Bacillus subtilis, and Pseudomonas aeruginosa. The study demonstrates the viability of Br-based ILs in biopolymer processing and materials engineering, though additional functionalization may be necessary to improve bioactivity.*

Keywords: ionic liquids; cellulose; activated carbon, green synthesis; biopolymer

1. INTRODUCTION

The growing urgency of environmental challenges, including global warming and resource depletion, has intensified interest in renewable biomass for sustainable production of fuels, chemicals, and materials [1–3]. Green composites made from biodegradable polymers such as cellulose and starch are particularly attractive due to their renewability and compatibility [4]. Cellulose, the most abundant biopolymer in nature, is composed of β-(1→4)-linked glucose units and has wide industrial applications [5–6]. Starch, being inexpensive and readily available, is also commonly used to enhance the mechanical properties of cellulose-based composites due to their polysaccharide compatibility [4].

Cellulose's applications in biomedical fields—particularly in wound dressings—stem from its favorable water absorption and liquid transport properties [7–8]. However, its poor mechanical strength limits its direct clinical use, which can be addressed through starch incorporation. Activated carbon, known for its high surface area and bacterial adsorption capacity [10–11], has been explored to improve the biological function of cellulose composites, potentially serving as odor-controlling or antimicrobial dressings [7].

Due to strong hydrogen bonding, cellulose is challenging to dissolve and modify using conventional solvents [12–17]. Ionic liquids (ILs) have emerged as promising green solvents owing to their thermal stability, low volatility, and recyclability [18–22]. In this study, pyridinium-based ILs were employed for cellulose dissolution and regeneration, followed by composite film fabrication with starch and activated carbon.

2. METHODOLOGY

2.1 Materials

Pyridine, various alkyl bromides (1-bromobutane, 2-bromobutane, 2-bromo-2-methylpropane, 1-bromohexane, 1-bromooctane, benzylbromide), sodium acetate, microcrystalline cellulose, activated carbon, and potato starch were used as received from commercial sources. Organic solvents (diethyl ether, dichloromethane) and nitrogen gas (99.99%) were locally sourced.

2.2 Synthesis of Br-based Ionic Liquids

Br-based pyridinium ionic liquids were synthesized via nucleophilic substitution by heating pyridine (10.0 mmol) with respective alkyl bromides (11.0 mmol) (n-C_4 to C_8, sec-C_4, t-C_4, and Bn) in a 25 mL Pyrex™ tube until single-phase solutions formed. The benzyl derivative was synthesized at room temperature due to spontaneous reaction.

2.3 Anion Metathesis

Anion exchange was conducted by heating the previously prepared Br-containing ionic liquids with sodium acetate (1:1.5 molar ratio) at 130 °C for 40–60 minutes. The resulting mixture was extracted with CH_2Cl_2, washed with diethyl ether, and dried under nitrogen.

2.4 Characterization of Ionic Liquids

FT-IR spectroscopy (PerkinElmer Spectrum 100) was used to identify functional groups over 4000–450 cm^{-1}. Thin-layer chromatography (TLC) was employed for polarity comparison, and $AgNO_3$ tests confirmed residual halide ions.

2.5 Preparation of Cellulose-Based Composite Films

Activated carbon (2, 6, 8 and 10 wt% with respect to the

biopoymer's content) was sonicated in pyridinium-based ionic liquids for 90 minutes. Cellulose or cellulose/starch blends were added and stirred at elevated temperature in an oil bath for 24 h until a homogeneous solution was obtained. The solution was cast into glass molds and soaked in water, with repeated water changes to remove residual ILs. Films were washed with distilled water, oven-dried at 50 °C for 3 h, and stored in a desiccator. Control cellulose films were prepared under the same conditions without activated carbon.

2.6 Film Characterization and Antimicrobial Testing

FT-IR (Thermo Fisher Nicolet 510) and SEM-EDS (JEOL JSM-6510LA) were used for structural and morphological analysis of the synthesized films. Antimicrobial activity was assessed via the paper disc diffusion method using standard bacterial and fungal strains from Economic Development Board-Industrial Technology Development Institute (EDB-ITDI) Microbial Culture Collection, DOST in Bicutan, Taguig City.

3. RESULTS AND DISCUSSIONS

3.1. Synthesis of Pyridinium-based Ionic Liquid

The general reaction for the synthesis of Br-based ionic liquids and all results are presented in Scheme 1 and Table 1, respectively.

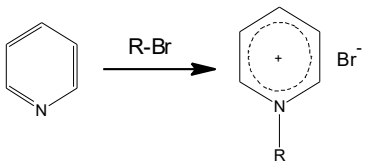

R= *n*-C4, *sec*-C4, *t*-C4, C6, C8, and Bn (benzyl)

Scheme 1. The general reaction for the synthesis of Br-based ionic liquids.

In summary, six ionic liquids based on pyridine were synthesized. The synthesized ionic liquids were generally yellowish in color, passed through a solid state, except for [C_6py]Br and [C_8py]Br, and gradually liquefied at room temperature over a range of six days to two weeks duration. [C_6py]Br and [C_8py]Br were liquids after heating as they were expected to have lower melting point. An increase in the alkyl chain (at some point n=4-10) decreases the melting temperature of the salt since the additional rotational degrees of freedom enhances the molar volume as well as chain flexibility of the cation [23-24].

Table 1. Percent Yield for the Synthesis of Br-based Ionic Liquids

Alkyl Bromide Used	Ionic Liquid	%Yield
1-bromobutane	[*n*-C_4py]Br	94.09 ± 3.68
sec-bromobutane	[*s*-C_4py]Br	39.56 ± 0.07
t-butylbromide	[*t*-C_4py]Br	9.56 ± 3.19
1-bromohexane	[C_6py]Br	86.55 ± 9.76
1-bromooctane	[C_8py]Br	89.15 ± 3.03
benzylbromide	[Bnpy]Br	97.49 ± 0.27

The reaction between pyridine and alkyl bromide proceeds through nucleophilic substitution, S_N2, which favors less sterically hindered substrates since bulky substrates impede the back-side attack of the nitrogen to the electrophilic carbon of alkyl bromide. This was evident in Table 1 where product yield generally decreased as branching of the alkyl group increases from primaryto tertiary. The observed product yields are 94.09%, 39.56% and 9.56% for primary, secondary and tertiary butyl, respectively. Steric effect was also observed for longer chain substrates. Increasing the number of carbons from 1-bromobutane to 1-bromooctane resulted in increased steric hindrance which lowers the product yield for longer alkyl chain analogues. The observed product yields for 1-bromobutane, 1-bromohexane and 1-bromooctane are 94.09%, 86.55% and 89.15%, respectively.

From the given preliminary data, [*n*-C_4py]Br was selected as the medium for cellulose dissolution and anion metathesis reaction since it afforded better yield compared to the other synthesized ionic liquids. Although [Bnpy]Br furnished better product yield (about 97.49%) than [*n*-C_4py]Br, the former took more time to liquefy making it as time-inefficient medium. Meanwhile, the results of the anion metathesis reaction are shown in Table 2.

Table 2. Percent Yield for the Anion Metathesis of 1-butylpyridinium Bromide

Run	Ionic Liquid	Heating conditions		% Yield
		Temp., °C	Time, min	
1	[*n*-C_4py] [OAc]	130	40	75.86 ± 5.06
2		130	50	80.11 ± 2.55
3		130	60	94.49 ± 2.16

The reaction was stopped initially after 40 minutes since the mixture turned slightly orange at this point indicating the progress of the reaction. The reaction mixture was also subjected to longer reaction time to determine the effect of reaction time on product yield for the anion metathesis reaction. During anion metathesis, reaction time played a critical role in the reaction as shown in Figure 3, in that prolonging the reaction time from 40 minutes to 60 minutes.

3.1. Characterization of Pyridinium-based Ionic Liquids

The resulting FT-IR spectra and band assignments for pyridine, Br-based ionic liquid and OAc-based ionic liquid are shown in Figure 1 and Table 3, respectively. Pyridine shows aromatic C-H vibrations in the region 3150 – 3000 cm^{-1} [25]. These bands were found at 3074, 3049 and 3020 cm^{-1} and shifted into slightly lower frequencies in the spectra for both Br-based and OAc-based ILs. This shifting of bands might have resulted from the weakened aromaticity in the pyridinium ring. It is known that quaternization of pyridine partially disrupts the aromaticity of pyridine ring. This was further manifested in the disappearance of aromatic C-C aromatic vibrations in spectra of prepared ionic liquids. It is also worth noting that an intense and broad band signal for -OH group was observed at 3403 cm^{-1} for Br-based ILs and 3443 cm^{-1} for OAc-based ILs. This band suggests the formation of the hydrated salt, [n-C_4py][anion]·xH_2O [26]. Pyridinium salts are known to

be extremely hygroscopic and without special drying procedures and completely inert handling, water is omnipresent in ionic liquids.

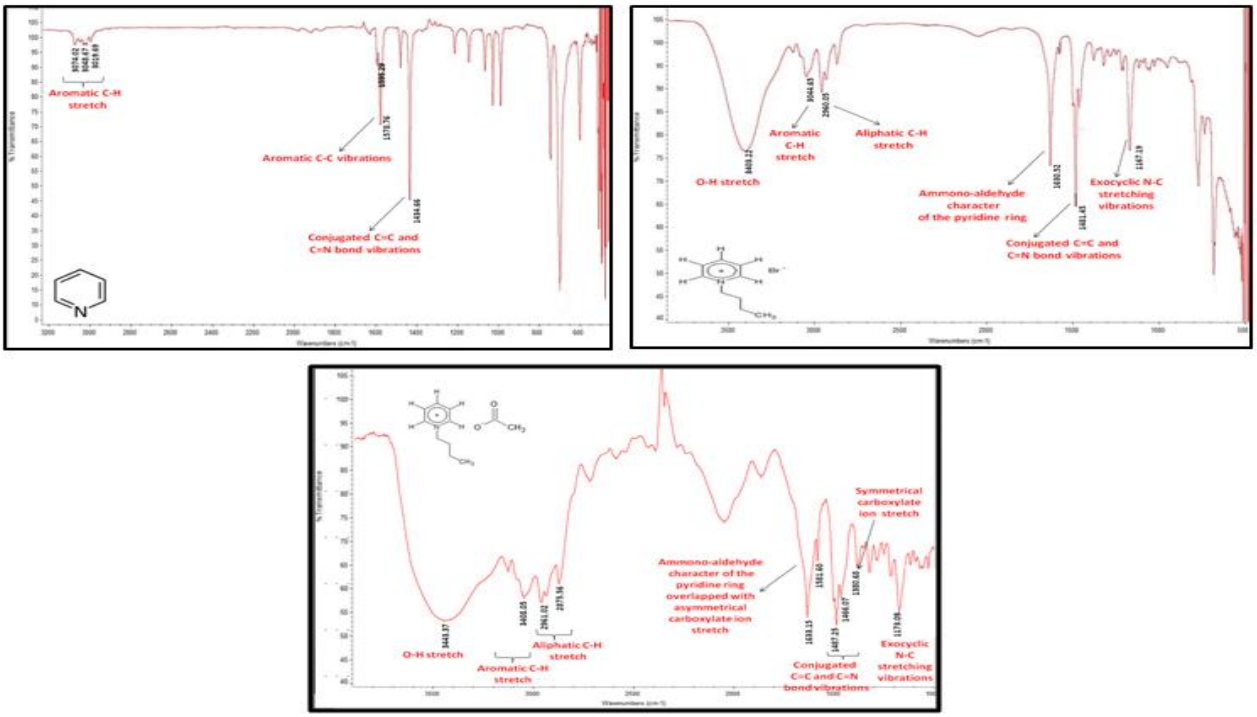

Fig. 1. FT-IR spectra of (a) neat pyridine, (b) Br-based and (c) OAc-based ionic liquid with its characteristic absorption peaks.

Table 3. Band Assignments for Neat Pyridine and Pyridinium-Based ILs [27]

Sample	Band assignment							
	Aromatic C-H stretch	Aromatic C-C vibrations	Conjugated C=C and C=N bond vibrations	O-H stretch	Aliphatic C-H stretch	Ammono-aldehyde character of the ring	Exocyclic N-C stretch	Symmetrical carboxylate ion stretch
Neat pyridine	3074 3049 3020	1595 1579	1435	-	-	-	-	-
[n-C_4py]Br	3045	-	1481	3403	2960	1631	1167	-
[n-C_4py][OAc]	3048	-	1487 1466	3443	2961 2876	1633* 1582*	1173	1381

*overlapped with Asymmetrical carboxylate ion stretch

The Br-based has shown a strong band at 1631 cm^{-1} which does not appear in the spectrum of pyridine. This band has been assigned to the ammono-aldehyde character of the pyridine ring, acquired because of quaternization [27]. The presence of an unshared pair of electrons in the sp^2 orbital of the nitrogen atom and existence of the C=N bond can be considered as an ammono-aldehyde system. The same absorption band was observed for the OAc-based ILs at 1633 cm^{-1} and a small sharp peak at 1582 cm^{-1}. These bands could be the overlapped absorption peaks for the ammono-aldehyde character of the pyridine ring and asymmetrical stretch vibrations of carboxylate ion. It is known that carboxylate ion gives rise to two bands: a strong asymmetrical stretching band near 1650-1550 cm^{-1} and a weaker, symmetrical stretching band near 1400 cm^{-1} [28] which was found in the spectrum of OAc-based ILs at 1381 cm^{-1}. In addition, a strong, sharp band was observed at 1167 and 1173 cm-1 for Br- and OAc-based ILs, respectively, which may be assigned to exocyclic N-C stretching vibrations in N-alkylated pyridinium salts [29]. Meanwhile, bands observed at 1430 – 1480 cm-1 which were present in all spectra may be assigned to ring vibrations and conjugated C=C and C=N bond vibrations [27].

Furthermore, thin layer chromatographic (TLC) profiling of both Br-based and OAc-based ILs also revealed that the two ionic liquids have quite similar polarity after they were subjected to different solvent systems ranging from nonpolar hexane, polar ethanol and a series of mixtures of those solvents. Bromide impurity, however, was evident in OAc-based ILs as it showed AgBr precipitate when it was allowed to react with 0.1M $AgNO_3$. The halide-free preparation of this type of ionic liquid is significantly more difficult since this ionic liquid is completely miscible with water and so cannot be reextracted from aqueous solution with CH_2Cl_2 or other organic solvents making the removal of the halide ions by washing procedure with water not an option. Consequently, to synthesize such ILs of completely

halide-free quality, special procedures must be applied such as the use of an ion-exchange resin [30].

3.3 Preparation of Cellulose-based Composites Films

In order to dissolve cellulose, the inter and intramolecular hydrogen bonding interactions have to be disrupted. Swatloski *et al*. reported that high negatively charged concentration is very efficient in breaking down the networked hydrogen bonding and thereby dissolving cellulose. The choice of the anion in the ILs structure plays a critical in cellulose dissolution and regeneration in which Br-based ILs regenerated a better cellulose film compared to OAc-based ILs. This might be due to the comparatively weak negative charge of OAc as a result of the resonance stabilization of acetate anion. Hence, only Br-based ILs was used for further fabrication of cellulose-based composite films. The best reaction temperature for dissolution of the cellulose was chosen from the range 90-110 ºC since most of the studies conducted for cellulose dissolution using ionic liquids were done at this temperature range [12-17]. Cellulose film regenerated at 90 °C was too brittle and very delicate to handle for characterization while there was no cellulose film regenerated at 110 °C since the dissolved cellulose solution readily coagulated before it was casted in the glass plate. On the other hand, cellulose film regenerated at 100 °C was found to be good enough to be handled for characterization. It was stiff, rigid and has paper-like surface and texture. Thus, the preparation of cellulose composites was done at 100 °C. Since the composite film products were intended for medical purposes as wound dressing, flexibility of the material is one of the criteria that must be met. The film regenerated at 100 °C was too rigid and stiff; hence potato starch together with the activated carbon was incorporated into the cellulose's matrix. The cellulose/starch composites have resulted to a more pliant and flexible film upon addition of starch up to 30 wt%. The granules of the starch became swollen and gelatinized when they are heated and addition of water further enhanced the gelatinization of starch. Water has been often used as a plasticizer for starch-containing composites to obtain the desirable product properties. However, further addition of the starch up to 50 wt% resulted into a slightly moist, brittle film. At this point, cellulose and starch were becoming thermodynamically immiscible due to their repelling response in the presence of excess water which led to poor adhesion between the two components and hence poor and irreproducible result.

Water content of the film was also a critical point in achieving good quality composite films. Further addition of the starch up to 50 wt% might have attracted too much water which resulted into composite film with poor quality. Incorporation of the starch to cellulose required more days for the film to dry due to the more hydrophilic nature of the starch. Reinforcements are also unique in that they will not affect the clarity of the polymer matrix. They will appear transparent since they are smaller than the wavelength of visual light [31]. Only a few percentages of these materials are normally incorporated (1–5%) into the polymer and the improvement is vast due to their large degree of surface area. Hence, the activated carbon was incorporated up to 10% only. However, incorporation of activated carbon both to cellulose and cellulose/starch mixture has resulted into brittle films with poor resistance to breakage. This might be due to the adsorptive properties of carbon. As the carbon adsorbed too much water, poor quality composite films were produced.

3.4 Characterizations of Cellulose-based Composites Films

3.4.1 FT-IR Spectroscopy Results

The FT-IR spectrum of the cellulose film product is depicted in Figure 2. The spectrum shows broad band characteristic at 3416.44 cm cm^{-1}. This is attributed to the O–H stretch in cellulose structure. The peaks at 1487.91 cm^{-1} and 2961.72 cm^{-1} are assigned to CH_2 symmetric bending and C–H stretching vibration respectively. The C–O-C asymmetrical stretching vibration peaks are situated at 1164.77 and 1110.00 cm^{-1}. The band around 1633.88 cm^{-1} could also be assigned to the absorbed water 'bending' vibrations [32-33].

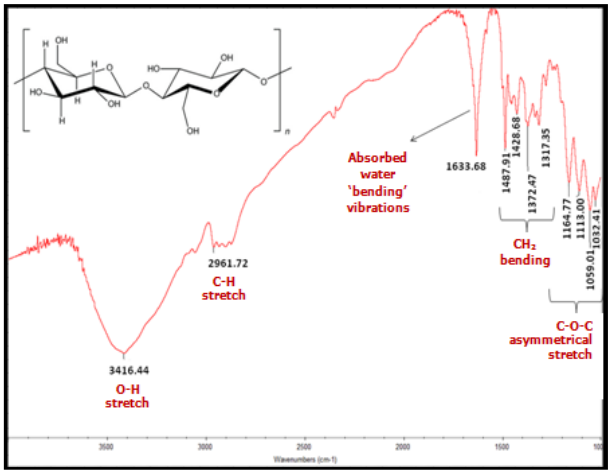

Fig. 2. FT-IR Spectrum of the prepared cellulose film product with its characteristic absorption peaks.

The FT-IR spectra of the cellulose films with potato starch are presented in Figure 3a-b. The composite films containing the cellulose and starch exhibited almost the same FTIR spectra as the cellulose film due to the chemical similarities between starch and cellulose. However, the position of the band intensities shifted to lower wave numbers compared to that of pure cellulose film peak. For instance, the –OH stretch shifted from 3416.44 to 3414.68 cm^{-1} in the composite films containing 10 wt% starch. This shift of band suggests that there is an increase of intermolecular hydrogen bonding by the addition of starch. This result is ascribed to the phenomenon that when polymers are compatible and a distinct interaction, *i.e.* hydrogen bonding or dipolar interaction, exists between the chains of cellulose matrix and starch, providing the changes of FT-IR spectra on the composites, e.g. band shifts and broadening [34]. Initially, pure activated carbon was subjected to FT-IR spectroscopy. Graphite-like structures (noncrystalline) are believed to be responsible for the absorptions at 1617.69 cm-1 and 1384.20 cm^{-1} [35]. The frequencies of the two broad infrared bands are in excellent agreement with the frequencies of the two laser-Raman lines found for various carbons: 1600 and 1360 cm^{-1}. The laser-Raman spectra are the same for coals, carbons and

graphites [33]. The broad band at 3414.75 cm^{-1} might be due to the –OH stretch in adsorbed water. Presence of

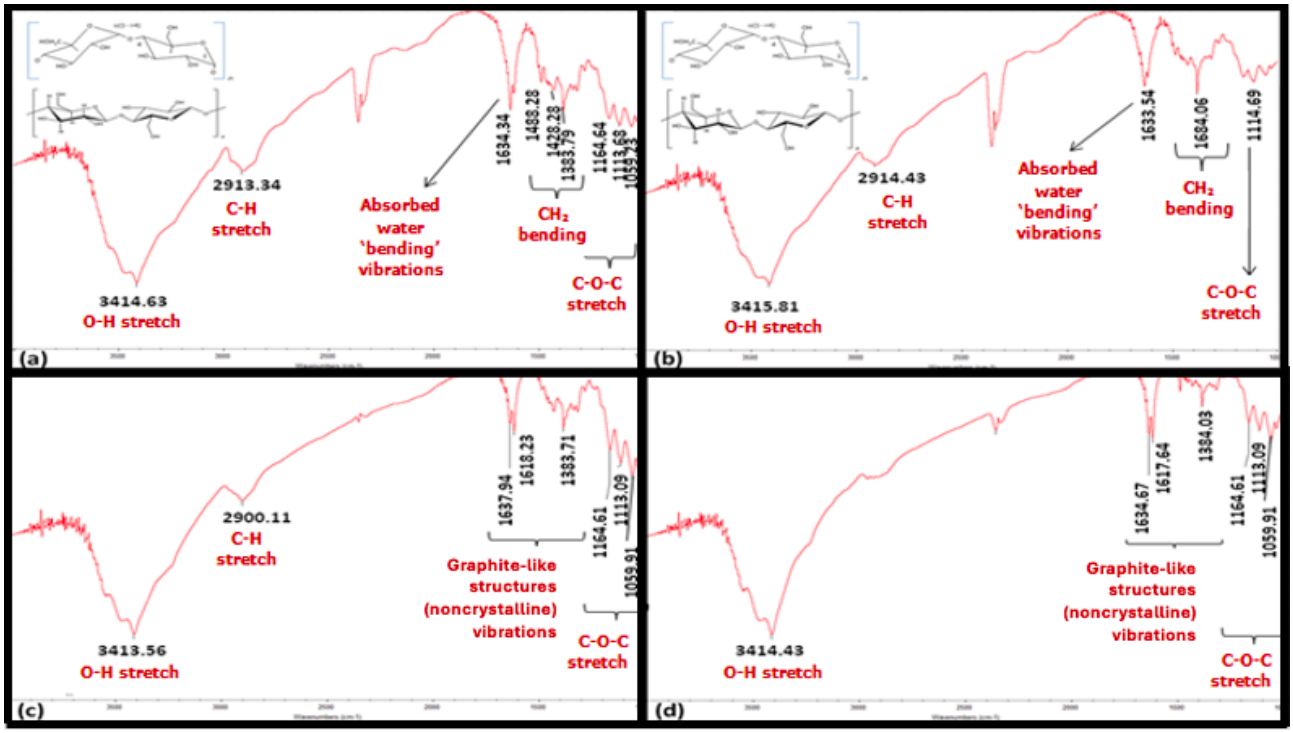

Fig. 3. FT-IR Spectra of the cellulose/starch composite film products containing (a) 10 % starch, (b) 20% starch, (c) 8 wt% and (d) 10 wt% activated carbon with its characteristic absorption peaks.

these unique peaks assigned only to activated carbon suggests incorporation of activated carbon on the composite films. The FT-IR spectra for cellulose/activated carbon composite films are shown in Figure 3c-d. Observations have shown that the characteristic peaks of the composites consist of activated carbon and cellulose characteristic absorption peaks. This is suggestive that there is incorporation of activated carbon in the composite films. Composite films containing smaller amount of activated carbon showed absorption peaks similar to pure cellulose films and no unique bands for activated carbon were detected. It is also worth observing that the CH_2 bending disappeared as more activated carbon was added into cellulose's matrix. This may be due to various factors. One of which is the entrapment of activated carbon in the tangled of cellulose fibers and remain between fibers of cellulose even during the process of regeneration. There is no chemical bond between cellulose and activated carbon since activated carbon is an inert substance. The trapped AC may have masked and restricted the CH_2 bending vibrations of the cellulose. Moreover, the presence of impurities on the composite films may have also an effect on the disappearance of CH_2 bending in the resulting FT-IR spectra. Trapped impurities could impose restrictions on the CH_2 bending vibrations of cellulose. The same absorption peaks were observed for the cellulose/starch/activated carbon composite films, as shown in Figure 9, where the characteristic absorption peaks assigned for activated carbon were detected and CH_2 bending vibrations vanished at higher activated carbon content (6 – 10 wt%).

3.4.2 Scanning Electron Microscopy Results

The topography of the prepared composite films was analyzed by SEM coupled with Energy Dispersive X-ray Spectroscopy (EDS). The regeneration process of cellulose resulted in irregular microcrystals together with amorphous areas (Fig. 5-a). The heterogeneity of the shape and size in this sample might be due to the high energy involved during dissolution and regeneration process [36]. Addition of starch into the cellulose matrix resulted into more ordered, sheet-like morphology (Fig. 10 b-e). This sheet-like morphology is consistent with the composite obtained by Wan et al. [37] where bacterial cellulose was incorporated into starch plasticized with glycerol via a solution impregnation method. The more structured morphology was manifested in the cellulose/starch films where there is an improvement (visually observed) after the addition of starch. Moreover, the 5000x magnification micrograph of cellulose/starch film (70/30) revealed that the spherical, gelatinized starch molecules appear to be embedded in the cellulose matrix, organized in bundles and well adhering to the matrix, as shown in Figure 5b. On the other hand, addition of activated carbon both to cellulose and cellulose/starch composite resulted to flake-like morphology with fiber pull-out indicating poor interfacial adhesion as indicated in Figure 5c. The added activated carbon particles are interposed between the polymer chains reducing the polymer–polymer interaction which are accompanied by the increase in the intermolecular space (free-volume), altering carbon adhesion to the polymer [38]. The decrease in mechanical properties of the composite is in good accordance with the results of Indriyati. *et al*. where the presence of more activated carbon in the composite led to less bacterial cellulose network binding. These observations were also manifested in the prepared cellulose/activated carbon and cellulose/starch/activated carbon films in which the addition of activated carbon resulted to films with poor quality.

Elemental analysis of cellulose and cellulose/starch composite films was also conducted, and the results were summarized in Table 4 and 5. The trace of Pt detected was from the sample coating during sample preparation for SEM-EDS analysis. It is also worth noting that no Nitrogen atom was detected suggesting that there is complete removal of ionic liquids after addition of water. The presence of Br might be due to the side reaction

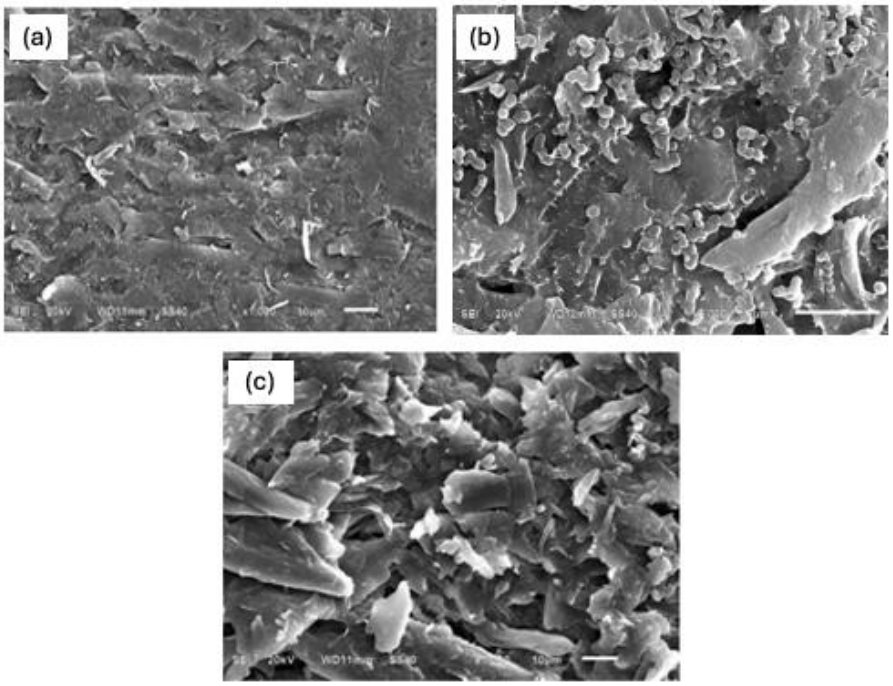

Fig. 5. SEM micrographs of cellulose-based composite film products: (a) cellulose/starch, 90/10; (b) cellulose/starch, 70 /30; and (c) cellulose/starch (70/30) with 6% AC.

between cellulose and bromide ion cementing the bromide in the surface of cellulose. Cellulose has several main sites in the glucose residues that can be considered for its modification. First, the C-1 and C-4 regions are of interest in degradation processes and regarding the reducing end-groups of the chains. Second, the ring oxygen atom and that of the glycosidic linkage play some part in intermolecular interactions, although not in covalent derivatization. Finally, the three hydroxyl groups in each glucose residue unit are particularly relevant. They can enter all well-known classical reactions, such as oxidation reactions, etherification, acylation, and deoxyhalogenation [39].

Table 4. Elemental Analysis of Cellulose and Cellulose/Starch Composite Films

Test Samples	%Atom			
	C	O	Br	Pt
Cellulose Film	84.73	12.26	2.67	0.33
Cellulose/Starch Film (90:10)	81.49	18.74	1.17	0.49
Cellulose/Starch Film (80:20)	82.55	15.06	1.76	0.63
Cellulose/Starch Film (70:30)	84.29	13.42	1.77	0.52
Cellulose/Starch Film (60:40)	82.52	15.20	1.60	0.68

Moreover, EDS detected the added activated carbon on the composite film products as shown in Table 5 where there is sudden increase in the carbon percentage from 84.73% to 86.19% after 2 wt% of activated carbon was incorporated into cellulose's matrix. Much more increase in the carbon's percentage was observed after 6 wt% of activated carbon was added into cellulose/starch composite.

Table 5. Elemental Analysis of Cellulose-Based Composite Films

Test Samples	%Atom			
	C	O	Br	Pt
Cellulose Film	84.73	12.26	2.67	0.33
Cellulose/Activated Carbon (2 wt%)	86.19	10.05	3.23	0.53
Cellulose/Starch (70:30) with activated carbon (6 wt%)	88.53	6.88	3.63	0.96

3.5 Antimicrobial Activity Evaluation of Cellulose-based Composite Films

The antimicrobial assay was used in this study for qualitative screening only and any clearing around the disc was considered a positive result. The in vitro antibacterial and antifungal activity evaluation of cellulose-based composites films which included pure cellulose film, cellulose/starch films and cellulose/activated carbon films were done by the paper disc diffusion method using representative test organisms: E. coli and P. aeruginosa (Gram -); B. subtilis and S. aureus (Gram +); A. flavus and A. niger (molds) and S. cerevisiae and C. albicans (yeasts). No antibacterial and antifungal activity evaluation was done on cellulose/starch/activated carbon films since the resulting films are too flaky and very delicate for disc preparation. Results revealed that the cellulose-based composite film products exhibited no significant growth-inhibitory

activity against the representative test organisms. Such inactivity of cellulose-based composite films towards the tested eight microorganisms could have been due to several factors. These include the particularly large size or structure of the tested molecules and their solubility which may hinder or even prevent its diffusion through agar. Furthermore, the presence of impurities on the cellulose-based composite films may have altered the bioactivity of activated carbon rendering the composite films inactive towards the tested microorganisms.

4. CONCLUSION

In this research work, cellulose-based composite films were prepared without using very harsh solvent systems. The results show that pyridinium-based ionic liquid may be a good medium for cellulose dissolution and regeneration. However, an ionic liquid containing a more negatively charged anion is needed for cellulose dissolution for the efficient disruption of inter- and intra-hydrogen bonding of cellulose. In the physico-chemical characterization of the film, FT-IR spectroscopy confirmed the compatibility of cellulose and starch as well as the incorporation of activated carbon in composite films. SEM images revealed well dispersion of gelatinized starch in cellulose matrix resulting into more ordered, sheet-like morphology. Addition of the starch markedly improved the fundamental physical and mechanical properties of the cellulose-based composite films. The finest film was obtained after addition of starch at 30 wt% ratio while addition of activated carbon particles reduced the polymer–polymer interaction resulting into films with poor quality. Moreover, in vitro antimicrobial activity evaluation of cellulose-based composite films screening revealed that all of the prepared films exhibited no significant growth-inhibitory activity against the representative test microorganisms.

5. REFERENCES

[1] Zhang, Y.H.P., Ding, S.Y., Mielenz, J.R., Cui, J.B., Elander, R.T., Laser, M., Himmel, M.E., McMillan, J.R. & Lynd, L.R. (2007). Fractionating recalcitrant lignocellulose at modest reaction conditions, Biotechnology and Bioengineering 97(2): 214-223.

[2] Ogaki, Y., Shinozuka, Y., Hatakeyama, M., Hara, T., Ichikuni, N. &Shimazu, S. (2009). Selective production of xylose and xylo-oligosaccharides from bamboo biomass by sulfonatedallophane solid acid catalyst, Chemistry Letters 38 (12): 1176-1177.

[3] Zhang, M.J., Qi, W., Liu, R., Su, R.X., Wu, S.M. & He, Z.M. (2010). Fractionating lignocellulose by formic acid: Characterization of major components, Biomass & Bioenergy 34(4): 525-532.

[4] Averous, L. and Boquillon, N. 2004. Biocomposites based on plasticized starch: thermal and mechanical behaviours. Carbohydrate Polymers. 56, 111-122.

[5] Xie, H.,King,A.,Kilpelainen, I., Granstrom,M., &Argyropoulos, D. S. (2007). Thorough chemical modification of wood-based lignocellulosic materials in ionic liquids. Biomacromolecules, 8, 3740–3748.

[6] Zhong C., Wang C., Huang F., Jia H., Wei P. Wheat straw cellulose dissolution and isolation by tetra-n-butylammonium hydroxide. Carbohydrate Polymers 94 (2013) 38– 45.

[7] Mogosanu, G. and Grumezescu, A. Natural and synthetic polymer for wounds and burns dressing. International Journal of Pharmaceutics 463 (2014) 127-136.

[8] Shezad, O., Khan, S., Khan, T., & Park, J. K. (2010). Physicochemical and mechanical characterization of bacterial cellulose produced with an excellent productivityin static conditions using a simple fed-batch cultivation strategy. Carbohydrate Polymers, 82, 173–180

[9] Maria, L. C. S., Santos, A. L. C., Oliveira, P. C., & Valle, A. S. S. (2010). Preparation andantibacterial activity of silver nanoparticles impregnated in bacterial cellulose.Polímeros: Ciência e Tecnologia, 20, 72–77.

[10] Percival, S.L., and Walker, J.T. 1999. Potable water and biofilms: a review of the public health implications. Biofoul. 14:99 115.

[11] Quinlivan, A., L. Li and Knappe, D. 2005. Predicting Adsorption Isotherms for Aqueous Organic Micropollutants from Activated Carbon and Pollutant Properties. Water. Res., 39:1663 1673

[12] A.J. de Menezes, D. Pasquini, A.A.D.S. Curvelo, A. Gandini, Cellulose 16 (2009) 239–246.

[13] O.A. El Seoud, A. Koschella, L.C. Fidale, S. Dorn, T. Heinze, Biomacromolecules 8 (2007) 2629–2647.

[14] T. Heinze, R. Dicke, A. Koschella, A.H. Kull, E.A. Klohr, W. Koch, Macromolecular Chemistry, Physics 201 (2000) 627–631.

[15] S. Zhu, Y. Wu, Q. Chen, Z. Yu, C. Wang, S. Jin, Y. Ding, G. Wu, Green Chemistry 8 (2006) 325–327.

[16] L. Zhang, D. Ruan, J. Zhou, Industrial Engineering Chemistry Research 40 (2001) 5923–5928.

[17] L. Yan, Z. Gao, Cellulose 15 (2008) 789–796.

[18] H. Olivier-Bourbigou, L. Magna, D. Morvan, Applied Catalysis A: General 373 (2010) 1–56.

[19] R.D. Rogers, K.R. Seddon, Science 302 (2003) 792–793.

[20] R.P. Swatloski, S.K. Spear, J.D. Holbrey, R.D. Rogers, Journal of the American Chemical Society 124 (2002) 4974–4975.

[21] S. Mahmoudian, M.U. Wahit, A.F. Ismail, A.A. Yussuf, Carbohydrate Polymers 88 (2012) 1251–1257.

[22] A. Fallah-Bagheri, A.A. Saboury, L. Ma'mani, M. Taghizadeh, R. Khodarahmi, S. Ranjbar, M. Bohlooli, A. Shafiee, A. Foroumadi, N. Sheibani, A.A. Moosavi-Movahedi, International Journal of Biological Macromolecules 51 (2012) 933–938.

[23] Holbrey, J. D., Seddon, K. R., J.Chem.Soc., Dalton Trans. 1999, 2133.

[24] Hardacre, C., Holbrey, J. D., Katdare, S. P., & Seddon, K. R. (2002). Alternating copolymerisation of styrene and carbon monoxide in ionic liquids. *Green Chemistry*, *4*(2), 143-146.

[25] Kline Jr, C. H., & Turkevich, J. (1944). The vibrational spectrum of pyridine and the thermodynamic properties of pyridine vapors. Journal of Chemical Physics, 12(7), 300-309.

[26] P. Wasserscheid, T. Welton, Ionic Liquids in Synthesis, second ed., WILEY-VCH,Weinheim, 2008.

[27] M. Katcka, T. Urbanski. Infrared Absorption Spectra of Quaternary Salts of Pyridine. Bulletin De L'academie, Polonaise Des Sciences. Serie des sciences chimiques. Volume XII, No. 9, 19S4

[28] Siverstein, R.M., and Webster, F.X., Spectrometric Identification of Organic Compounds, 6th ed. John Wiley & Sons, Inc. 1998.
[29] R. N. Jones and C. Sandorfy, The application of infrared and Raman spectrometry to the elucidation of molecular structure, in W. West, ed., Chemical applications of spectroscopy (Vol. IX of A. Weissberger, ed., Technique of organic chemistry), Interscience, New York — London, 1956, pp. 247—580.
[30] H. Waffenschmidt, dissertation, RWTH Aachen, 2000
[31] Alexandra M, Dubois P. Polymer-layered silicate nanocomposites: preparation, properties and uses of a new class of materials. Mater Sci Eng, R 2000;28:1–63.
[32] Kolpak, F. J. & Blackwell, J. (1976). Determination of the Structure of Cellulose II. Macromolecules, Vol.9, No.2, pp. 273-278, ISSN 0024-9297.
[33] Yano, S., Hatakeyama, H. & Hatakeyama, T. (1976). Effect of hydrogen bond formation on dynamic mechanical properties of amorphous cellulose. Journal of Applied Polymer Science, Vol.20, No.12, pp. 3221-3231, ISSN 1097-4628.
[34] Prachayawarakorn, J., Sangnitidej, P. and Boonpasith, P. 2010. Properties of thermoplastic rice starch composites reinforced by cotton fiber or low-density polyethylene. Carbohydrate Polymers. 81, 425-433.
[35] Friedel, R. A. and Queiser, J. A. Infrared And Raman Spectra Of Intractable Carbonaceous Substances--Reassignments in Coal Spectra. Pittsburgh Energy Research Center, Bureau of Mines U.S. Department of the Interior, Pittsburgh, Pa. 15213.
[36] Panaitescu, D., Frone, A.N., Ghiurea, M., Spataru, C., Radovici,C. and Iorga, M. Properties of Polymer Composites with Cellulose Microfibrils. National Institute of Research and Development in Chemistry and Petrochemistry, Romania.
[37] Wan, Y.Z., Luo, H.L., He, F., Liang, H., Huang, Y., and Li, X.L. (2009) Mechanical, moisture absorption, and biodegradation behaviours of bacterial cellulose fibre-reinforced starch biocomposites. Composites Science and Technology, 69(7–8), 1212–1217.
[38] Indriyati, R. Yudianti, and L. Indrarti. Development of Bacterial Cellulose/Activated Carbon Composites Prepared by In Situ and Cast-drying Method. Asian Transactions on Basic and Applied Sciences (ATBAS ISSN: 2221-4291) Volume 02 Issue 05.
[39] R. H. Attala and A. Isogai, Recent developments in spectroscopic and chemical characterization of cellulose, in S. Dumitriu (Eds.), Polysaccharides, Structural Diversity & Functional Diversity, Marcel Dekker, New York, 2005, pp. 123–157.